Trajectory Planning of Biped Robot Using Linear Pendulum Mode for Double Support Phase

Maki Shibuya, Tomoyuki Suzuki and Kouhei Ohnishi, *Fellow, IEEE*

Department of System Design Engineering, Keio University, Yokohama, Japan
shibu@sum.sd.keio.ac.jp tomoyuki@sum.sd.keio.ac.jp ohnishi@sd.keio.ac.jp

Abstract— **Double support phase is important for biped robots to achieve stable walking. In this research, a simple trajectory planning method using Linear Pendulum Mode (LPM) is proposed for double support phase. A biped robot is modeled by a pendulum in LPM. The walking stability is assured when the supporting point of LPM is set in the specific area. The area is shown clearly with Zero Moment Point (ZMP) in this paper.**

LPM is able to be applied to various motions since LPM uses a simple pendulum model. In this paper, a stop motion is described, for example. A pendulum has the dynamism that the COG velocity in the horizontal direction becomes 0 at particular points. LPM realizes natural stop motions using the dynamism.

Keywords— **biped robot, linear pendulum mode, double support phase, trajectory planning, stop motion**

I. Introduction

A. Background

Bipedal locomotion is divided into two terms; single support phase and double support phase.

Many control methods for single support phase have been proposed for biped robots to achieve dynamic walking. One of those methods was proposed by Shimoyama[1]. In this method, the dynamic walking was realized using a stilts type biped robot. Another method is "Linear Inverted Pendulum Mode (LIPM)" proposed by Kajita and Tani[2][3]. A biped robot is modeled by an inverted pendulum in the method. LIPM is used widely for trajectory planning in single support phase since it makes control of biped robots easy.

In the meanwhile, there is not much control methods for double support phase. Sometimes double support phase is ignored. However, the walk in double support phase is able to improve walking stability. Kajita[3] said that the addition of double support phase to LIPM diminished the loss of COG velocity on switching supporting legs. Hurusyo and Yamada[4] proposed a control method for double support phase. Biped robots kicked the ground in double support phase in this method. Angular momentum of robots at the start of single support phase was adjusted by the kick. Toda et al.[5] proposed another method. The shock of a swing leg on landing was reduced in double support phase. In these methods, walking stability in single support phase was improved.

The walk in double support phase contributes the stable walking as above stated. It is desirable to adopt double support phase into walking. This paper, therefore, proposes a easy-to-use control method for double support phase.

B. Related works

Some of the conventional researches into double support phase are introduced, here.

Kajita et al.[6] showed a simple trajectory planning method in double support phase. In the method, the COG position was given by quartic function of time. Although this method was simple, walking stability was not taken into account.

Making a point of walking stability, Sano et al.[7] proposed some methods. Torque of both ankle joints is distributed so that the sum of both torque becomes minimum in double support phase. Ito et al.[8] proposed another method that COG is moved in double support phase controlling the center of pressure of each feet. Although these methods may realize stable walking, it is hard to imagine instinctively generated COG trajectory. Easiness of imagining COG trajectory is important to plan natural walking motions since the COG movement represents the look of walking. Another method was proposed by Mitobe et al.[9]. ZMP was defined on the imaginary ceiling and was controlled by operating ankle joint torque. With this ZMP movement, COG was moved and controlled. This method needs the reaction force value of the high accuracy force sensor for calculating ZMP. It is because the value gauged by force sensor has much noise.

In the meantime, as one of researches into stop motions, the other proposition in this paper, there is the method proposed by Morisawa et al.[10]. In this method, the algorithm of the emergency stop motion is shown. The trajectory is determined so that the travel distances of COG and ZMP are minimized. Kaneko[11] et al. presented another algorithm for judgment on suspension and suspending motions. These methods cost a large amount of calculation.

C. Overview of the proposed method

The conventional control methods for double support phase satisfy either of the easiness of trajectory planning or assurance of walking stability. This paper, therefore, proposes the trajectory planning method that combines both of simplicity of planning and guarantee of walking stability. The method is named "Linear Pendulum Mode (LPM)". Easiness of trajectory planning of LPM is owing to a pendulum model. LPM is easy to be used with another motion since LPM is simple and needs small amount of calculation. Walking stability is assured by the relationship between

1-4244-0136-4/06/$20.00 ©2006 IEEE

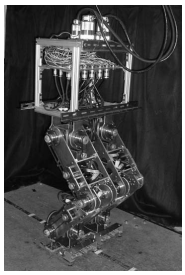

Fig. 1. Overview of the robot

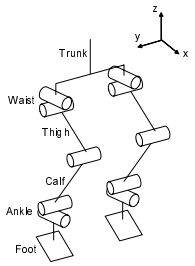

Fig. 2. 3D model of the robot

TABLE I
PARAMETERS OF LINKS

	Mass [kg]	Length [m]	COG from upper joint [m]
Trunk	10.2	0.40	0.200
Waist	2.6	0.00	-0.200
Thigh	3.5	0.30	0.126
Calf	3.4	0.30	0.095
Ankle	2.6	0.00	-0.020
Foot	2.0	0.12	0.023

ZMP and a pendulum. The area of supporting point of LPM to assure walking stability is shown clearly in this research.

LPM is applied to various motions in double support phase, the motions at the beginning and the end of a walking, and so on. In this paper, a stop motion is described. LPM realizes natural stop motions by using the dynamism of a pendulum. This method is simple and needs a small amount of calculation.

The effectiveness of the proposed method is demonstrated by simulations and experiments.

D. Composition of this paper

This paper is composed as follows: In section Ⅱ, the modeling and kinematics of the biped robot are shown. LPM is proposed in section Ⅲ and its stability is described in section Ⅳ. In section Ⅴ and Ⅵ, the results of simulations and experiments are shown respectively. The application of LPM to a stop motion is proposed in section Ⅶ. Finally, we conclude this paper in section Ⅷ.

II. Modeling

A. Modeling

The overview of the biped robot that we use in this research is shown in Fig. 1 and the 3D model is shown in Fig. 2. The robot has 10 DOF; 4 in frontal plane and 6 in sagittal plane. In this research, it is assumed that the biped robot is constrained in sagittal plane. The biped robot is modeled assuming the mass of each link exists in the COG of the link. A base link is set on the trunk. Table I shows the parameters of each link.

B. Kinematics

At first, direct kinematics of the robot is shown. Following homogeneous transform matrix, ${}^nT_m$, is used for converting a link coordinate system Σ_m into Σ_n as (1).

$$\begin{bmatrix} {}^n\boldsymbol{P} \\ 1 \end{bmatrix} = \begin{bmatrix} {}^n\boldsymbol{R}_m & {}^n\boldsymbol{P}_m \\ 0 & 1 \end{bmatrix} \begin{bmatrix} {}^m\boldsymbol{P} \\ 1 \end{bmatrix} = {}^n\boldsymbol{T}_m \begin{bmatrix} {}^m\boldsymbol{P} \\ 1 \end{bmatrix} \tag{1}$$

${}^n\boldsymbol{P}$:Position in Σ_n. ${}^n\boldsymbol{P}_m$:Position of link m in Σ_n. ${}^n\boldsymbol{R}_m$:Rotation matrix from Σ_m to Σ_n. Σ_m and Σ_n represent the criterion coordinate system of link m and n respectively.

Next, inverse kinematics is explained. 3 DOF of COG position and 2 DOF of the base link attitude are controlled. Redundant 5 DOF are used for controlling the position and the attitude of the tip of the swing leg. The Joint angular acceleration reference values of the robot are calculated by following (2) and (3).

$$\ddot{\boldsymbol{\gamma}}^{ref} = \boldsymbol{J}_c^+ \ddot{\boldsymbol{x}}_c^{ref} + (\boldsymbol{I} - \boldsymbol{J}_c^+ \boldsymbol{J}_c)\tilde{\boldsymbol{J}}_t^+ (\ddot{\boldsymbol{x}}_t^{ref} - \boldsymbol{J}_t \boldsymbol{J}_c^+ \ddot{\boldsymbol{x}}_c^{ref}) \tag{2}$$

$$\tilde{\boldsymbol{J}}_t = \boldsymbol{J}_t \left(\boldsymbol{I} - \boldsymbol{J}_c^+ \boldsymbol{J}_c\right) \tag{3}$$

$\boldsymbol{x}_c$:COG position vector of a robot in world coordinate, Σ_W. $\boldsymbol{x}_t$:Tip position vector of a swing leg in Σ_W. $\boldsymbol{\gamma}$:Joint angle vector. $\boldsymbol{J}$:Jacobian matrix. Superscript ref and $+$ represent a reference value vector and an pseudo inverse matrix respectively.

III. Proposition of LPM

For stable and smooth walking, double support phase is important. In order to adopt double support phase into walking easily, this paper proposes simple trajectory planning method for double support phase. Additionally, proposed method assures walking stability. The method is named "Linear Pendulum Mode (LPM)". LPM becomes especially useful and easy-to-use when it is used with Linear Inverted Pendulum Mode (LIPM). LIPM is used for single support phase in this research. In this paper, the motion of the biped robot is considered only in sagittal plane.

A. LIPM in single support phase

The walk without double support phase is planed easily using LIPM like Fig. 3(a). In this case, the COG acceleration in horizontal direction has discontinuous point when the supporting legs are switched. That is caused by the assumption that the supporting legs are switched instantaneously. Fig. 3(b) shows the COG velocity in horizontal direction of the walking with LIPM. The discontinuous point of the COG acceleration is shown at $t = t_2$. The motions with the discontinuity of COG accelerarion tend to become unstable since robots are subjected to sharp force.

In order to avoid the impulsive force, a walking should have double support phase. COG acceleration is made continuous by smooth switching supporting legs in double support phase.

B. Introduction of LPM into walking with LIPM

The proposed method, LPM, uses a pendulum model shown in the shaded region of Fig. 4. A supporting point

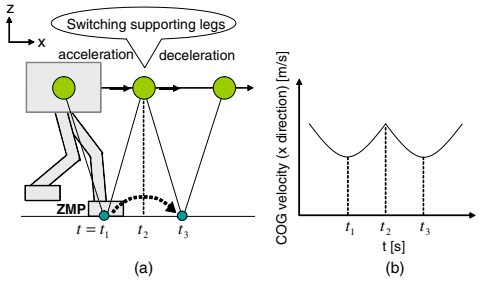

Fig. 3. COG position(a) and velocity(b) of a walking using LIPM

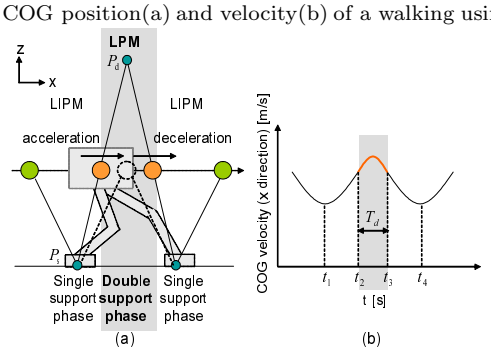

Fig. 4. COG position(a) and velocity(b) of a walking using LPM

is defined above a center of gravity (COG) of the robot. The velocity pattern is from acceleration to deceleration. This pattern is opposite to that of LIPM. Therefore, COG acceleration of LPM connects with that of LIPM smoothly when supporting legs are switched. The walking motion using LPM and LIPM is shown in Fig. 4.

The pendulum model is used in both of single and double support phase. In single support phase, the supporting point of LIPM is set on the ground. In double support phase, the supporting point is shifted above COG. Like this, the two modes, LPM and LIPM, are switched by the shift of the supporting points. With this method, the trajectory planning of the whole walk becomes very simple. It is easy to get the overview of walking condition after some steps or seconds. To forecast easily is important in walking trajectory planning.

C. Motion of LPM and LIPM

The COG position and velocity in LPM and LIPM are described, here. The origin of the coordinate system in LIPM and LPM is represented as O_s and O_d respectively. O_s and O_d are set on the each supporting point of pendulum model as shown in Fig 5 and Fig 6. The supporting points of LIPM and LPM are represented as P_s and P_d each. In both mode, COG movement is constrained on a particular line. x and z axes are defined in the horizontal and vertical direction respectively. (x_s, z_s) and (x_d, z_d) represent the position of COG in LIPM and LPM each.

C.1 Motion equation of LIPM

The model of LIPM is shown in Fig. 5. The motion equation is represented as (4).

$$M\ddot{x}_s = f\sin\theta = Mg\frac{x_s}{z_s} \tag{4}$$

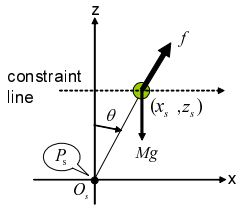

Fig. 5. Model of LIPM

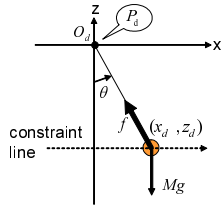

Fig. 6. Model of LPM

θ :Angle of the supporting leg from z axis. M :Mass of the whole robot. g :Acceleration of gravity. f :Reaction force from ground.

The COG position and velocity are derived as (5) and (6) by solving (4) with initial position, $x_s(0)$, and velocity, $\dot{x}_s(0)$. The characteristic frequency, ω_s, is represented as (7). In this paper, a constraint line of COG is set on horizontal line.

$$x_s(t) = \frac{\omega_s x_s(0) + \dot{x}_s(0)}{2\omega_s}e^{\omega_s t} + \frac{\omega_s x_s(0) - \dot{x}_s(0)}{2\omega_s}e^{-\omega_s t} \tag{5}$$

$$\dot{x}_s(t) = \frac{\omega_s x_s(0) + \dot{x}_s(0)}{2}e^{\omega_s t} + \frac{-\omega_s x_s(0) + \dot{x}_s(0)}{2}e^{-\omega_s t} \tag{6}$$

$$\omega_s = \sqrt{\frac{g}{z_s}} \tag{7}$$

C.2 Motion equation of LPM

The model of LPM is shown in Fig. 6. The motion equation is represented as (8).

$$M\ddot{x}_d = Mg\frac{x_d}{z_d} \qquad (z_d < 0) \tag{8}$$

Solving (8) with initial position, $x_d(0)$, and velocity, $\dot{x}_d(0)$, the COG position and velocity is derived. These are shown in (9) and (10). The characteristic frequency, ω_d, is represented as (11). In this paper, a constraint line of COG is set on horizontal line.

$$x_d(t) = \frac{\omega_d x_d(0) - j\dot{x}_d(0)}{2\omega_d}e^{j\omega_d t} + \frac{\omega_d x_d(0) + j\dot{x}_d(0)}{2\omega_d}e^{-j\omega_d t} \tag{9}$$

$$\dot{x}_d(t) = \frac{j\omega_d x_d(0) + \dot{x}_d(0)}{2}e^{j\omega_d t} + \frac{-j\omega_d x_d(0) + \dot{x}_d(0)}{2}e^{-j\omega_d t} \tag{10}$$

$$\omega_d = \sqrt{\frac{g}{z_d}} \tag{11}$$

From (4) and (8), the absolute values of the COG acceleration in LIPM and LPM are equal when $|\frac{x}{z}|$ in two modes are equal. Hence, P_d is set on the line that goes through P_s and COG like Fig. 7. With that, the accelerations of two modes are connected continuously when two modes are switched. The term of double support phase, T_d, is calculated by (12) with the initial COG condition, $(x_d(0), \dot{x}_d(0))$, and the end condition, $(x_d(T_d), \dot{x}_d(T_d))$.

$$T_d = \frac{1}{\omega_d}\arccos^{-1}\left(\frac{\omega_d x_d(0)x_d(T_d) + \frac{\dot{x}_d(0)\dot{x}_d(T_d)}{\omega_d}}{\omega_d x_d(0)^2 + \frac{\dot{x}_d(0)^2}{\omega_d}}\right) \tag{12}$$

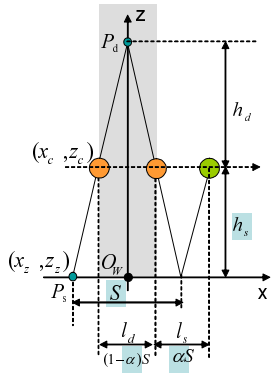

Fig. 7. Relation among parameters

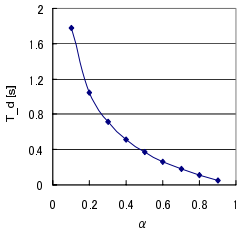

Fig. 8. Relation between α and T_d

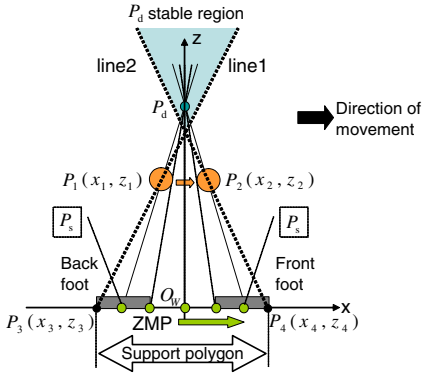

Fig. 9. ZMP of LPM

D. Timing of switching LPM and LIPM

The timing of switching LPM and LIPM is explained, here. The COG movement distances during single support phase and double support phase are represented as l_s and l_d respectively. h_s and h_d represent the distances between COG and P_s or P_d in z direction. These parameters are shown in Fig. 7. l_s and l_d are given with stride S and a parameter α like (13).

$$l_s = S - l_d = \alpha S \qquad (0 < \alpha < 1) \tag{13}$$

h_d is determined by h_s and α as (14).

$$h_d = \frac{1-\alpha}{\alpha} h_s \tag{14}$$

S, h_s and α are determined at will. However, S and h_s have the constraint that the robot must not become singular configuration. Therefore, the term of double support phase is controlled by modulating α. The change of T_d by α is shown in Fig. 8 when walking parameters are in Table III .

IV. Stability of LPM

In this section, the walking stability in LPM is described. The walking stability is determined by whether ZMP of a robot exists in support polygon or not.

At first, the ZMP position in LPM is derived. The origin of the world coordinate, O_W, is set at the middle point of both feet on the ground like Fig. 7. The ZMP position and COG position in LPM are represented as (x_z, z_z) and (x_c, z_c) in Σ_W respectively. x_z on the ground is calculated by (15) in the case that a robot is regarded as a mass point of COG[6].

$$x_z = \frac{1}{1-\alpha} x_c \tag{15}$$

(15) is given with (8) and (14). From (15), ZMP exists on the same straight line with P_d and COG as shown in Fig. 9. Therefore, ZMP shifts smoothly from the back foot to the front foot following the movement of COG.

Next, the region of P_d that ZMP exists in support polygon is shown clearly. The region is called P_d stable region in this paper. In Fig. 9, the robot moves to the right. The COG positions at the beginning and the end of double support phase are represented as $P_1(x_1, z_1)$ and $P_2(x_2, z_2)$ respectively. Support polygon in double support phase is from $P_3(x_3, z_3)$ to $P_4(x_4, z_4)$. P_3 and P_4 represent the heel of the back foot and the tip of the front foot each. The line1 goes through P_1 and P_3. The line2 goes through P_2 and P_4. The line1 and line2 make the shaded inverted triangle area shown in Fig. 9. This area is just P_d stable region and is given by (16). Since ZMP exists in support polygon throughout double support phase when P_d exists in the area. The P_d has to be set in the area.

$$\begin{cases} z > \frac{z_1 - z_3}{x_1 - x_3} x + \frac{x_1 z_3 - x_3 z_1}{x_1 - x_3} \\ z > \frac{z_2 - z_4}{x_2 - x_4} x + \frac{x_2 z_4 - x_2 z_4}{x_2 - x_4} \end{cases} \tag{16}$$

In this research, P_d is determined on the point where particular two lines intersect. One is the line going through P_s on the back foot and P_1. The other is the line going through P_s on the front foot and P_2. With this, P_d is sure to exists in the P_d stable region. The walking stability in LPM, therefore, is always satisfied.

V. Simulation

In this section, the results of simulation with the proposed method are shown. In this research, we assumed that COG of LPM and LIPM were set at the waist of the robot. A spring-damper model was used as the model of the ground. For dynamics in simulation, the motion equation extended for a manipulator on mobile robot was used[13]. PD-controller and disturbance observer[12] were used for control system of simulation and experiment. The control parameters used in simulation are shown in Table II.

A. The walk only using LIPM

The simulation results of the walk only using LIPM are shown to compare with the proposed method. The walk parameters are shown in Table III. The response of the COG velocity and ZMP position in x direction are shown in Fig. 10 and Fig. 11 respectively. In the shaded region, the robot happened to be in double support since the swing leg landed earlier than estimated time. This early landing is caused by the modeling error of the robot. Although it is

TABLE II

CONTROL PARAMETERS

Control parameter		Simulation	Experiment
Position gain	K_p	2500	400
Velocity gain	K_v	100	40
Sampling time[s]	st	0.001	0.001
Disturbance Observer Cutoff frequency[rad/s]	g_{obs}	100	100

TABLE III

WALK PARAMETERS(SIMULATION)

Walk parameter		LIPM	LIPM and LPM
Single support phase[s]	T	3.0	3.0
Stride[m]	S	0.2	0.25
COG height[m]	z_s	0.55	0.55
α	α	-	0.3

TABLE IV

WALK PARAMETERS(EXPERIMENT)

Walk parameter		LIPM and LPM
Single support phase[s]	T	3.0
Stride[m]	S	0.15
COG height[m]	z_s	0.55
α	α	0.3

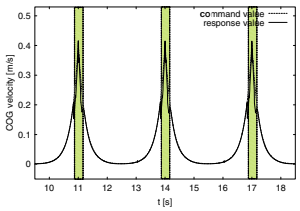

Fig. 10. COG velocity of LIPM (Simulation)

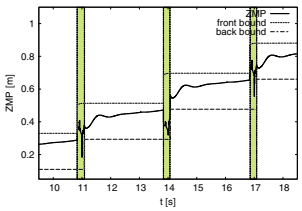

Fig. 11. ZMP of LIPM (Simulation)

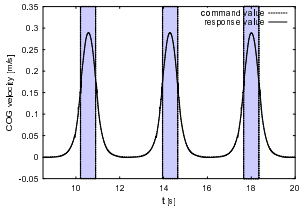

Fig. 12. COG velocity of LIPM and LPM (Simulation)

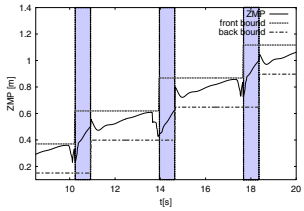

Fig. 13. ZMP of LIPM and LPM (Simulation)

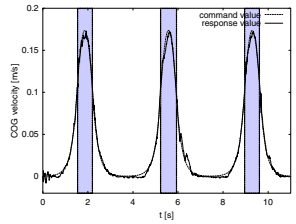

Fig. 14. COG velocity of LIPM and LPM (Experiment)

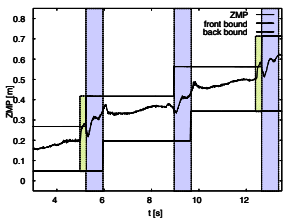

Fig. 15. ZMP of LIPM and LPM (Experiment)

assumed that the robot has the massless legs in LPM and LIPM, the real robot's legs have the mass.

From Fig.10, the top of the velocity curve is sharp. At that time, ZMP changes rapidly from Fig.11. These mean the acceleration of COG is discontinuous at that time.

B. The walk using LIPM and LPM

The simulation results of the walk using LIPM and LPM are shown. The walk parameters are shown in Table III. The response value of COG velocity and ZMP position in x direction is shown in Fig. 12 and Fig. 13 respectively. The shaded region represents double support phase. From Fig.12, the top of COG velocity curve is smooth. Adittionally, ZMP shifts forward smoothly in double support phase from Fig.13. These mean the discontinuity of COG acceleration was dissolved by LPM. With above, the effectiveness of the proposed method was demonstrated by simulation.

VI. EXPERIMENT

In this section, the effectiveness of the proposed method is demonstrated by experiments. The control parameters are shown in Table II and the walk parameters are shown in Table IV.

The response value of COG velocity is shown in Fig. 14. The shaded region represents double support phase. From Fig. 14, the top of COG velocity curve is smooth. The proposed method acted effectively to avoid the discontinuous point of COG acceleration.

ZMP response in x direction is shown in Fig. 15. In the region that diagonal lines were drawn, the robot is in double support by early landing of the swing leg as discussed previously. ZMP shifted from the back foot to the front foot in double support phase in Fig. 15. This means that the supporting legs are smoothly switched maintaining walking stability. Consequently, the effectiveness of the proposed method is demonstrated by an experiment.

VII. APPLICAION OF LPM TO STOP MOTION

A. Stop motion using LPM

LPM is applied to various motions in double support phase, the motions at the beginning and the end of a walking, and so on. It is because LPM uses a pendulum model and it is very simple model. As one of the applications of LPM, this paper focuses on the stop motion.

LPM has the point where the COG velocity in horizontal direction becomes 0, when COG goes far from P_d. Natural stop motions are able to be realized by using the dynamism that a pendulum stops at the point where its COG velocity becomes 0. In conventional methods, the special algorithm is used for stop motion and a large amount of calculation is needed. However, in proposed method, the same pendulum model and algorithm with usual walking is also applied to stop motions. This trajectory planning is very simple and has the merit that amount of calculation is small. Additionally, as shown in section IV, the stability during stop motions is able to be discussed clearly.

B. Algorithm of Stop motions

The procedure of the stop motion is explained. At first, the point where the velocity of COG becomes 0 is calcu-

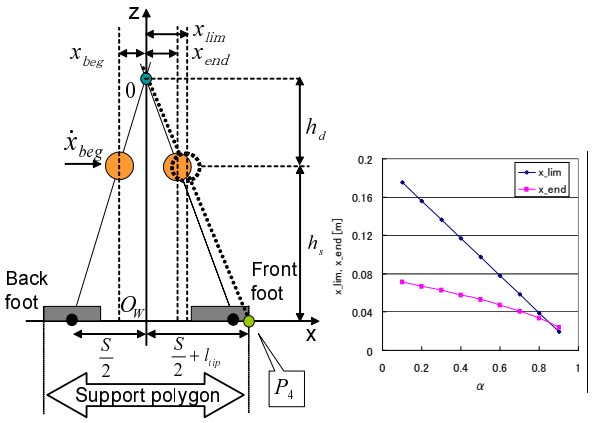

Fig. 16. Parameter in stop motion

Fig. 17. Relation between x_{lim} and x_{end}

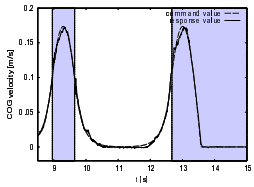

Fig. 18. COG velocity of stop motion (Experiment)

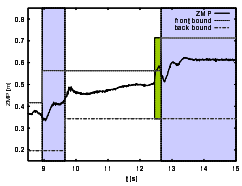

Fig. 19. ZMP of stop motion (Experiment)

lated. The orbital energy[6] of LPM is constant and is represented as (17).

$$\frac{1}{2}\dot{x}_d^2 + \frac{g}{2z_d}x_d^2 = E(\text{constant}) \tag{17}$$

E :Orbital energy of LPM. The COG position is represented as x_{end} when the COG velocity in x direction becomes 0. The COG position and velocity at the beginning of double support phase are represented as x_{beg} and $\dot{x}_{beg}$ respectively. Fig. 16 shows the COG movement of the stop motion. x_{end} is calculated by x_{beg} and $\dot{x}_{beg}$ as (18).

$$x_{end} = \sqrt{\frac{2h_d}{g}\left(\frac{1}{2}\dot{x}_{beg}^2 + \frac{g}{2h_d}x_{beg}^2\right)} \tag{18}$$

Next, it is checked whether ZMP exists in ZMP safety region when the robot stops at x_{end}. The position of COG is represented as x_{lim} when ZMP is on the front boundary P_4. x_{lim} is given by (19) from geometric relationship of Fig. 16.

$$x_{lim} = \frac{h_d}{h_s + h_d}\left(\frac{S}{2} + l_{tip}\right) \tag{19}$$

l_{tip} :Length from the ankle to the tip of the robots.

The relation between x_{lim} and x_{end} is shown in Fig. 17 when the walk parameters in Table IV are used. From Fig. 17, x_{end} is smaller than x_{lim} when α is less than about 0.9. With such α, the robot is able to stop naturally when the COG velocity becomes 0.

C. Experiment of stop motion

In this section, the experiment result of the stop motion using LPM is shown. The walk parameters are shown in Table IV. The COG velocity is shown in Fig. 18. The shaded part represents double support phase. From Fig. 18, the robot stops in the second double support phase with COG velocity 0.

The shift of ZMP in x direction is shown in Fig. 19. From Fig. 19, ZMP shifted and stopped in support polygon in double support phase. These results show that the robot stops naturally using LPM. The effectiveness of LPM in stop motion is shown.

VIII. Conclusions

In this paper, we proposed LPM into the trajectory planning for double support phase. LPM is very easy to plan a trajectory and ensures the walking stability since LPM uses a pendulum mode. Besides, LPM is able to realize a natural stop motion by using dynamism of a pendulum. We showed the effectiveness of these proposed methods by simulations and experiments.

References

[1] I. Shimoyama, "Dynamical Walking of Stilts Type Biped Locomotion," *Transactions of the Japan Society of Mechanical Engineers. C*, Vol.48, No.433, 1982, pp. 1445-1455.

[2] S. Kajita and K. Tani, "Study of dynamic walk control of a biped robot on rugged terrain. Derivation and application of the linear inverted pendulum mode," *The Society of Instrument and Control Engineers*, Vol.27, No.2, 1991, pp. 177-184.

[3] S. Kajita and K. Tani, "Dynamic Biped Walking Control on Rugged Terrain Using the Linear Inverted Pendulum Mode," *The Society of Instrument and Control Engineers*, Vol.31, No.10, 1995, pp. 1705-1714.

[4] J. Furusyo and M. Yamada, "Dynamic Control of Biped Locomotion Robot in Consideration of Angular Mormentum," *The Society of Instrument and Control Engineers*, Vol.22, No.4, 1986, pp. 451-458.

[5] K. Toda, T. Furuta and K. Toyama, "Biped Gait for Humanoids -Introduction of Double-Leg Supporting Phase for Stabilization-," *in Procceding of the 18rd Annual Conference of the Robotics Society of Japan,* 2000

[6] S. Kajita, Humanoid Robot, Ohmsha, Japan, 2005, pp. 135-136.

[7] A. Sano, J. Furusyo and Y. Ikami, "Control of Torque Distribution in Biped Systems during Double-Support Phase," *The Society of Instrument and Control Engineers*, Vol.26, No.9, 1990, pp. 1066-1073.

[8] S. Ito, H. Asano, M. Yamamo and H. Kawasaki, "A Weight Shift by Control of Center of Pressure of Ground Reaction Forces in Biped Double Support Phase," *Journal of the Robotics Society of Japan*, Vol.22, No.4, 2004, pp. 535-542.

[9] S. Kaneko, K. Mitobe, M. Yamamo and Y. Nasu, "Control of the Walking Robots based on the ZMP Defined on the Ceiling," *Journal of the Robotics Society of Japan*, Vol.23, No.3, 2005, pp. 370-375.

[10] M. Morisawa, S. Kajita, K. Harada, K. Fujiwara, F. Kanehiro, K. Kaneko and H. Hirukawa, "Emergency Stop Algorithm for Walking Humanoid Robots," *in Procceding of IEEE/RSJ International Conference on Intelligent Robotics and System,* 2005

[11] K. Kaneko, F. Kanehiro, M. Morisawa, S. Kajita, K. Fujiwara, K. Harada, and H. Hirukawa, "Motion Suspension System for Humanoid," *in Procceding of the 23rd Annual Conference of the Robotics Society of Japan,* 2005

[12] K. Ohnishi, "Robust Motion Control by Disturbance Observer," *Journal of the Robotics Society of Japan*, Vol.11, No.4, 1997, pp. 486-493.

[13] K. Yoshida, "The SpaceDyn: A MATLAB Toolbox for Space and Mobile Robots," *Journal of the Society of Instrument and Control Engineers*, Vol.38, No.2, 1999, pp. 138-143.